



UNIVERSITY
OF WOLLONGONG
AUSTRALIA

University of Wollongong
Research Online

Australian Institute for Innovative Materials - Papers

Australian Institute for Innovative Materials

2009

Crystal structure and electronic and thermal properties of $\text{TbFeAsO}_{0.85}$

N Kaurav

National Dong Hwa University Taiwan

Y.T Chung

National Dong Hwa University Taiwan

Y.K Kuo

National Dong Hwa University Taiwan

R S Liu

National Taiwan University

T S Chan

National Synchrotron Radiation Research Center, Taiwan

See next page for additional authors

Publication Details

Kaurav, N, Chung, Y, Kuo, Y, Liu, R, Chan, T, Chen, J, Lee, J, Sheu, H, Wang, P, Dou, SX, Lee, S, Shi, Y, Belik, A, Yamaura, K & Takayama-Muromachi, E (2009), Crystal structure and electronic and thermal properties of $\text{TbFeAsO}_{0.85}$, Applied Physics Letters, 94(19), pp. 192507-1-192507-3.

Research Online is the open access institutional repository for the University of Wollongong. For further information contact the UOW Library:
research-pubs@uow.edu.au

Crystal structure and electronic and thermal properties of TbFeAsO_{0.85}

Abstract

The crystal structure and the electronic and thermal properties of a high-quality polycrystalline TbFeAsO_{0.85} sample made by a high-pressure technique are investigated. The crystal structure, as determined by synchrotron X-ray powder diffraction, possesses a tetragonal unit cell (space group: $P4/nmm$) with lattice parameters of $a=b=3.8851$ Å and $c=8.3630$ Å. In order to elucidate the electronic structure and oxidation states of corresponding elements, X-ray absorption near-edge structure (XANES) spectra are presented. The XANES spectra confirm that the oxidation states of Fe, As, and Tb in the TbFeAsO_{0.85} sample are $\sim\text{Fe}^{2+}$, $\sim\text{As}^{3-}$, and $\sim\text{Tb}^{3+}$, respectively, which are consistent with the previously reported band structure calculations. The n -type character of the charge carriers as revealed from XANES spectra is corroborated by the negative sign of the Seebeck coefficient (S) in the present study. The heat capacity (C_p) measurement shows an anomaly in the vicinity of the superconducting transition temperature ($T_c=42.5$ K), which confirms the bulk nature of the superconductivity in this material.

Keywords

Crystal, structure, electronic, thermal, properties, TbFeAsO

Disciplines

Engineering | Physical Sciences and Mathematics

Publication Details

Kaurav, N, Chung, Y, Kuo, Y, Liu, R, Chan, T, Chen, J, Lee, J, Sheu, H, Wang, P, Dou, SX, Lee, S, Shi, Y, Belik, A, Yamaura, K & Takayama-Muromachi, E (2009), Crystal structure and electronic and thermal properties of TbFeAsO_{0.85}, Applied Physics Letters, 94(19), pp. 192507-1-192507-3.

Authors

N Kaurav, Y.T Chung, Y.K Kuo, R S Liu, T S Chan, J.M Chen, J.F Lee, H.S Sheu, Xiaolin Wang, S X. Dou, Sung-Ik Lee, Y.G Shi, A.A Belik, K Yamaura, and E Takayama-Muromachi

Crystal structure and electronic and thermal properties of TbFeAsO_{0.85}

N. Kaurav,¹ Y. T. Chung,¹ Y. K. Kuo,^{1,a)} R. S. Liu,^{2,a)} T. S. Chan,³ J. M. Chen,³ J.-F. Lee,³ H.-S. Sheu,³ X. L. Wang,⁴ S. X. Dou,⁴ S. I. Lee,⁵ Y. G. Shi,⁶ A. A. Belik,⁶ K. Yamaura,⁶ and E. Takayama-Muromachi⁶

¹Department of Physics, National Dong Hwa University, Hualien 97401, Taiwan

²Department of Chemistry, National Taiwan University, Taipei 106, Taiwan

³National Synchrotron Radiation Research Center, Hsinchu 300, Taiwan

⁴Institute for Superconducting and Electronic Materials, University of Wollongong, New South Wales 2522, Australia

⁵National Creative Research Initiative Center for Superconductivity, Department of Physics, Sogang University, Seoul 121742, Republic of Korea

⁶National Institute for Materials Science, Tsukuba, Ibaraki 305-0044, Japan

(Received 28 December 2008; accepted 24 April 2009; published online 15 May 2009)

The crystal structure and the electronic and thermal properties of a high-quality polycrystalline TbFeAsO_{0.85} sample made by a high-pressure technique are investigated. The crystal structure, as determined by synchrotron X-ray powder diffraction, possesses a tetragonal unit cell (space group: $P4/nmm$) with lattice parameters of $a=b=3.8851$ Å and $c=8.3630$ Å. In order to elucidate the electronic structure and oxidation states of corresponding elements, X-ray absorption near-edge structure (XANES) spectra are presented. The XANES spectra confirm that the oxidation states of Fe, As, and Tb in the TbFeAsO_{0.85} sample are $\sim\text{Fe}^{2+}$, $\sim\text{As}^{3-}$, and $\sim\text{Tb}^{3+}$, respectively, which are consistent with the previously reported band structure calculations. The n -type character of the charge carriers as revealed from XANES spectra is corroborated by the negative sign of the Seebeck coefficient (S) in the present study. The heat capacity (C_p) measurement shows an anomaly in the vicinity of the superconducting transition temperature ($T_c=42.5$ K), which confirms the bulk nature of the superconductivity in this material. © 2009 American Institute of Physics.

[DOI: 10.1063/1.3136764]

Layered rare-earth metal oxypnictides (LaFeAsO) have emerged as materials of exceptional scientific interest due to the discovery of high-temperature superconductivity in this family.¹ The strong interplay between structural, magnetic, and superconducting properties in this class of materials has led to the closing of comparisons with the physics of superconducting copper oxides.^{2,3} It has been also recognized that FeAs-based compounds could be a promising thermoelectric candidate in refrigeration applications around liquid nitrogen temperature.⁴ These aspects have motivated several studies replacing La atoms by other lanthanide atoms, resulting in elevated critical temperatures (T_c) from 26 to 56 K, the highest reported so far.^{5,6} These quaternary superconductors have a rather simple structure, consisting of alternating $[\text{Fe}_2\text{As}_2]^{2-}$ and $[\text{Ln}_2\text{O}_2]^{2-}$ layers with eight atoms in a tetragonal unit cell ($P4/nmm$), where the $[\text{Fe}_2\text{As}_2]^{2-}$ layer is thought to be responsible for superconductivity, while the $[\text{Ln}_2\text{O}_2]^{2-}$ layer provides charge carriers, resembling the similar layered structure found in high- T_c cuprates.⁷

Superconductivity in LaFeAsO has been also realized by doping with F atoms or by producing oxygen vacancies instead, which can create more carriers in the charge reservoir layer.^{8,9} Thus, the stacking of these layers and the ionic states of constituent atoms both play decisive roles in the transport and superconducting properties. Understanding the structural, electronic, and thermal properties would be an important step toward realizing the proposed technological scenario for this class of materials. Although the electrical and

magnetic properties (with $T_c=42$ K) of polycrystalline TbFeAsO_{0.85} samples have been described elsewhere recently,^{9,10} in this letter, we focus on the electronic structure and oxidation states by measuring X-ray absorption near-edge structure (XANES) spectra. Moreover, we have independently confirmed the value of T_c from a heat capacity anomaly, which is consistent with the previously reported resistivity results.⁹ The thermal conductivity and Seebeck coefficient of TbFeAsO_{0.85} are also discussed. Our results indicate that the anomalous behavior of the Seebeck coefficient cannot be accounted for by the conventional metallic picture alone.

The polycrystalline TbFeAsO_{0.85} used in this work was prepared by a high-pressure method.^{9,10} Synchrotron x-ray diffraction (XRD) patterns were recorded at the BL01C2 beam line of the National Synchrotron Radiation Research Center (NSRRC). Structural refinements were carried out by using the General Structural Analysis System (GSAS) program.¹¹ The XRD pattern of TbFeAsO_{0.85} can be indexed based on a tetragonal unit cell (space group: $P4/nmm$) with lattice parameters $a=b=3.8851$ Å and $c=8.3630$ Å, similar to those of the $\text{ReFeAsO}_{1-\delta}$ (Re=rare-earth metal) samples in Ref. 8.

The Fe, As K -edge, and Tb L_3 -edge XANES spectra were recorded in transmission mode at a wiggler BL17C beamline. The O K -edge XANES measurements were performed with a 6 m high-energy spherical grating monochromator BL20A beamline in the fluorescence-yield mode. Seebeck coefficient and thermal conductivity measurements were simultaneously performed by means of a heat pulse technique. Detailed descriptions of the experimental tech-

^{a)}Authors to whom correspondence should be addressed. Electronic addresses: ykkuo@mail.ndhu.edu.tw and rslu@ntu.edu.tw.

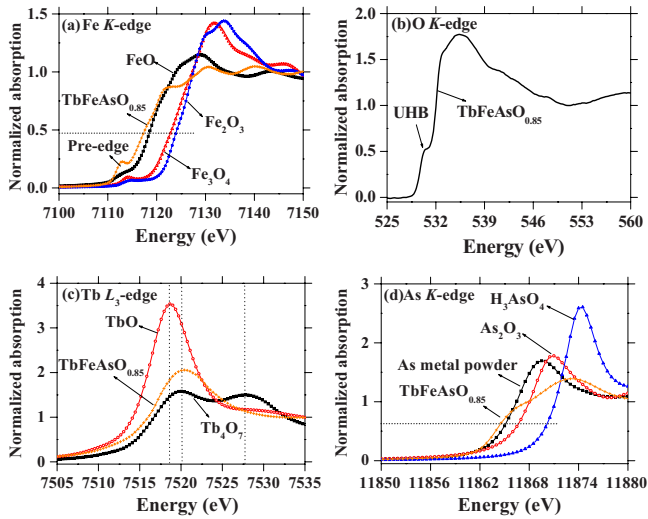


FIG. 1. (Color online) (a) Fe K -edge XANES spectra of $\text{TbFeAsO}_{0.85}$, along with three standards: FeO (Fe^{2+}), Fe_3O_4 ($\text{Fe}^{2.67+}$), and Fe_2O_3 (Fe^{3+}). The dashed line at the absorption coefficient value of 0.5 is included to elucidate the chemical shift. (b) O K -edge XANES spectrum of $\text{TbFeAsO}_{0.85}$. (c) Tb L_3 -edge XANES spectra of $\text{TbFeAsO}_{0.85}$, with two standards: TbO (Tb^{2+}) and Tb_4O_7 (Tb^{3+} and Tb^{4+} mixture). (d) As K -edge XANES spectra of $\text{TbFeAsO}_{0.85}$ with three standards: As metal powder (As^{0+}), As_2O_3 (As^{3+}), and H_3AsO_4 (As^{5+}).

niques for thermal measurements can be found elsewhere.¹²

The Fe K -edge XANES spectra of $\text{TbFeAsO}_{0.85}$, along with three standards, FeO (Fe^{2+}), Fe_3O_4 ($\text{Fe}^{2.67+}$), and Fe_2O_3 (Fe^{3+}), are shown in Fig. 1(a). It is well known that the chemical shift of the main absorption edge to lower energies with decreasing valence of transition metals is a powerful tool for probing the unknown valence of a transition metal.¹³ In Fig. 1(a), a dashed line at the absorption coefficient value of 0.5 is included to elucidate the chemical shift. The $\text{TbFeAsO}_{0.85}$ spectrum is close to, but slightly shifted to, lower energies relative to the FeO (Fe^{2+}) spectrum. This evidence indicates that the electron configuration of Fe in the $\text{TbFeAsO}_{0.85}$ sample is a mixture of the basic d^6 (Fe^{2+}) state and the d^7 (plus ligand hole) configuration in the ground state. Moreover, the pre-edge peak at around 7112 eV represents the $1s \rightarrow 3d$ transition, which is a dipole forbidden process. Such a pre-edge feature in $\text{TbFeAsO}_{0.85}$ is much stronger than in other standard compounds due to the local tetragonal ligand field allowing dipole transitions into $3d$ related states.¹³ The O K -edge XANES spectrum of $\text{TbFeAsO}_{0.85}$ is displayed in Fig. 1(b). The appearance of the broad peak located at about 530 eV indicates the n -type character of the charge carriers. Such an observation is also reported for other n -type high- T_c superconductive copper oxide $(\text{Nd,Ce})_2\text{CuO}_{4+\delta}$ systems, which is ascribed to transitions into the O $2p$ states hybridized with the upper Hubbard band (UHB).^{14,15}

In Fig. 1(c), Tb L_3 -edge XANES spectra of $\text{TbFeAsO}_{0.85}$ and two standard TbO (Tb^{2+}) and Tb_4O_7 (Tb^{3+} and Tb^{4+} mixture) compounds are shown. It is well known that the Tb_4O_7 spectrum has two broad peaks centered at ~ 7522 and ~ 7530 eV, reflecting the inhomogeneous, mixed-valence nature of the sample.¹⁶ The peak position at ~ 7522 eV in the Tb L_3 -edge XANES spectrum of $\text{TbFeAsO}_{0.85}$, together with the absence of a second absorption peak, indicates that the Tb is neither a tetravalent nor a mixed valence but is instead essentially Tb^{3+} in this sample. Figure 1(d) shows the

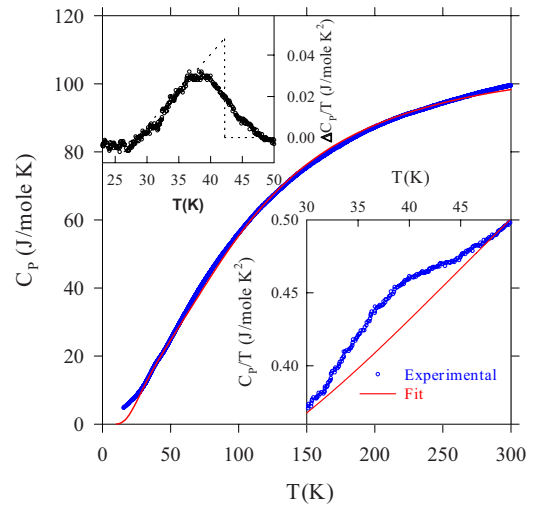


FIG. 2. (Color online) The temperature dependence of the specific heat for $\text{TbFeAsO}_{0.85}$. The solid red line represents the fit using the Einstein model. The lower and upper insets show the plots of C_p/T vs T and $\Delta C_p/T$ vs T , respectively. The dashed line in the lower inset shows the Debye model fit.

As K -edge XANES spectrum of the $\text{TbFeAsO}_{0.85}$ sample with three standards, including As powder (As^0), As_2O_3 (As^{3+}), and H_3AsO_4 (As^{5+}). In view of the absorption coefficient value of ~ 0.5 , the As K -edge spectrum of $\text{TbFeAsO}_{0.85}$ is clearly shifted to lower energies relative to that of As powder, indicating that the oxidation number of As in $\text{TbFeAsO}_{0.85}$ is negative. Considering the valence of Fe and Tb, we assume that the oxidation state of As in $\text{TbFeAsO}_{0.85}$ is approximately 3^- .

In Fig. 2 we show the specific heat (C_p) of $\text{TbFeAsO}_{0.85}$ in the temperature range of 20–300 K. The observed room temperature value is $C_p(300 \text{ K}) \approx 100 \text{ J/mol K}$, which is close to the Dulong–Petit limiting value and is consistent with previous results.^{17–19} This signifies that the bulk of the contribution indeed comes from the vibrational heat capacity in this temperature range. The solid line in Fig. 2 represents a fitting of the C_p using the Einstein model, $C_E = 3rR \sum a_i [x_i^2 e^{x_i} / (e^{x_i} - 1)^2]$, where $x_i = h\nu_E / k_B T_i$. Three optical phonons ($i=1, 2, 3$) having the Einstein frequencies $h\nu_E / k_B = 122, 330, \text{ and } 430 \text{ K}$ and relative occupations a_i were used. It is interesting to note that our phonon frequencies are nicely matched with those seen in a recent Raman measurement²⁰ and in lattice dynamical calculations.^{21,22}

Since the Debye model is more applicable in the low-temperature regime, we have further estimated the specific heat between 20 and 60 K with a cutoff frequency given by the Debye temperature $\theta_D = 330 \text{ K}$, and this is plotted as a dashed line in the lower inset of Fig. 2. The deduced value of the Debye temperature is comparable with reported data.^{17–19,22} The most apparent feature in our C_p result is that an abnormality of the heat capacity is clearly observed in the vicinity of the superconducting transition temperature (T_c), which has been absent in earlier reports on FeAs-based superconductors so far.^{17–19} The change in the entropy, $\Delta S = 0.31 \text{ J/mol K}$, associated with the superconducting transition was then obtained by subtracting the lattice part from the experimental data. In the upper inset of Fig. 2, $\Delta C_p/T$ is plotted as a function of T within a narrow temperature interval of 25–50 K at around T_c . Here, the excess heat capacity (ΔC) is obtained by subtracting the estimated background

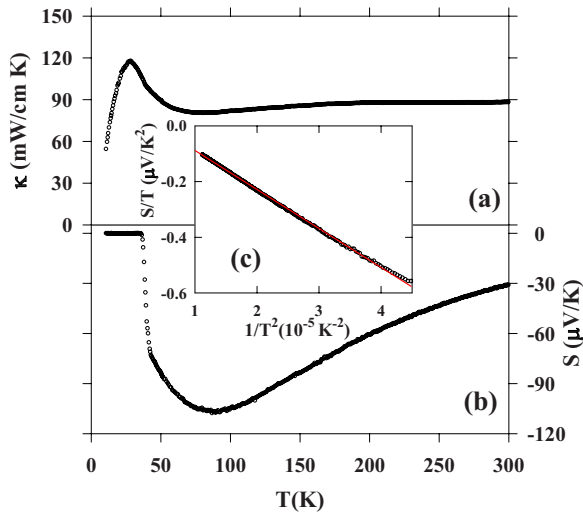


FIG. 3. (Color online) (a) Thermal conductivity vs temperature for $\text{TbFeAsO}_{0.85}$. (b) Seebeck coefficient as a function of temperature for $\text{TbFeAsO}_{0.85}$. (c) S/T is found to be linear with $1/T^2$ above 150 K.

from the total measured C_p . By considering the entropy conservation between the superconducting and normal states, we have deduced that the mean field heat capacity jump has a value of 2.2 J/mol K and that the superconducting transition $T_c = 42.5$ K, which is consistent with resistivity measurements.⁹

In Fig. 3, we show the variations of the Seebeck coefficient $S(T)$ and the thermal conductivity $\kappa(T)$ with temperature for $\text{TbFeAsO}_{0.85}$. The negative sign of S is consistent with the electronlike conduction mechanism. The absolute value of S increases from 31 $\mu\text{V/K}$ at room temperature to a maximum value (S_{max}) of 107 $\mu\text{V/K}$ at 90 K and then decreases sharply toward zero when the temperature reaches T_c [Fig. 3(b)]. The temperature variation and absolute value of S are similar to those reported for iron-based superconductors.^{18,19,23,24} It should be pointed out here that these materials exhibit an exceptionally large S and a rather low electrical resistivity at low temperatures, which is thought to be advantageous for low-temperature refrigeration applications.⁴ We have tried to fit our experimental results for the conventional diffusion and phonon drag component to S , written as $(aT+b/T)$, as is applicable to high- T_c cuprates.²⁵ In Fig. 3(c), it can be seen that S/T is linear with $1/T^2$ above 150 K, and there is a departure from a simple metallic behavior below this temperature. It has been argued that the freezing-out of Umklapp processes could have resulted in the dome-shaped feature in $S(T)$ and the enhancement of S in the case of high- T_c cuprates.²⁵ The effects of large anisotropy and the shape of the Fermi surface are expected to have an impact on the population of phonon modes and, hence, Umklapp processes.²² Also, the appearance of a sharp low-temperature peak in the thermal conductivity data [Fig. 3(a)] further supports the necessity of an Umklapp process in the thermal transport. However, strong electron correlations and spin fluctuations should suppress the nonequilibrium effects in the phonon distribution function, resulting in a significant slackening of the phonon drag term. The band structure value of S of about 6.8 $\mu\text{V/K}$ provides additional arguments against the conventional metallic interpretation of S .²²

On the other hand, spin entropy could be another likely source of the anomalously large S in the FeAs-based superconductors. It is worth mentioning that the importance of spin entropy has been pointed out for large S in the Na_xCoO_2 system.²⁶ This indicates that a large absolute value of S can be realized when the thermal energy ($k_B T$) is much less than the on-site Coulomb repulsion U , and S can be approximately $\sim -k_B \ln 2/|e|$. Here, the $\ln 2$ term comes from the spin fluctuations of Fe^{2+} ions, and the estimated value of $|S| \sim 60 \mu\text{V/K}$ could account for about 60% of the observed S_{max} .

In summary, a high-quality polycrystalline $\text{TbFeAsO}_{0.85}$ sample was synthesized by a high-pressure method, and the crystal structure and the electronic and thermal properties were investigated. The XANES spectra confirm that the oxidation state of Fe, As, and Tb in the $\text{TbFeAsO}_{0.85}$ sample is $\sim \text{Fe}^{2+}$, $\sim \text{As}^{3-}$, and $\sim \text{Tb}^{3+}$, respectively. The specific heat measurement shows an anomaly in the vicinity of the superconducting transition temperature ($T_c = 42.5$), which confirms the bulk nature of the superconductivity in this material. The negative sign of the measured Seebeck coefficient signifies electronlike charge carriers, in good agreement with the XANES measurements. Our results indicate that the large S value cannot be explained by the conventional metallic picture alone, and spin entropy could be another likely source for the observed large Seebeck coefficient in FeAs-based superconductors.

The authors would like to thank the National Science Council of Taiwan for financially supporting this research under Contract Nos. NSC 97-2628-M-259-001-MY3 (Y.K.K) and NSC 97-2113-M-002-012-MY3 (R.S.L). This work is also partially supported by the Australian Research Council through a Discovery project, DP0558753, the Japan Science and Technology Agency (JST), TRIP of Japan, and the program of Accelerated Research of the Korea Science and Engineering Foundation of the Ministry of Science and Technology (MOST/KOSEF) of Korea.

¹Y. Kamihara *et al.*, *J. Am. Chem. Soc.* **130**, 3296 (2008).

²X. H. Chen *et al.*, *Nature (London)* **453**, 761 (2008).

³T. Y. Chen *et al.*, *Nature (London)* **453**, 1224 (2008).

⁴L. Pinsard-Gaudart *et al.*, *Phys. Status Solidi (RRL)* **2**, 185 (2008).

⁵C. Wang *et al.*, *Europhys. Lett.* **83**, 67006 (2008).

⁶R. H. Liu *et al.*, *Phys. Rev. Lett.* **101**, 087001 (2008).

⁷P. Quebe *et al.*, *J. Alloys Compd.* **302**, 70 (2000).

⁸Z. A. Ren *et al.*, *Europhys. Lett.* **83**, 17002 (2008).

⁹Y. G. Shi *et al.*, *J. Phys. Soc. Jpn. Suppl. C* **77**, 155 (2008).

¹⁰Y. G. Shi *et al.*, arXiv:0812.4907.

¹¹A. C. Larson and R. B. V. Dreele, "Generalized Structure Analysis System," Los Alamos National Laboratory Report No. LAUR 86-748, 1994.

¹²Y. K. Kuo *et al.*, *Phys. Rev. B* **64**, 125124 (2001).

¹³J. Wong *et al.*, *Phys. Rev. B* **30**, 5596 (1984).

¹⁴E. Pellegrin *et al.*, *Phys. Rev. B* **47**, 3354 (1993).

¹⁵R. S. Liu *et al.*, *Solid State Commun.* **118**, 367 (2001).

¹⁶U. Staub *et al.*, *Phys. Rev. B* **50**, 7085 (1994).

¹⁷Y. Kohama *et al.*, *Phys. Rev. B* **78**, 020512 (2008).

¹⁸A. S. Sefat *et al.*, *Phys. Rev. B* **78**, 104505 (2008).

¹⁹M. A. McGuire *et al.*, *Phys. Rev. B* **78**, 094517 (2008).

²⁰V. G. Hadjiev *et al.*, *Phys. Rev. B* **77**, 220505 (2008).

²¹L. Boeri *et al.*, *Phys. Rev. Lett.* **101**, 026403 (2008).

²²D. J. Singh *et al.*, *Phys. Rev. Lett.* **100**, 237003 (2008).

²³L. J. Li *et al.*, *Phys. Rev. B* **78**, 132506 (2008).

²⁴A. S. Sefat *et al.*, *Phys. Rev. B* **77**, 174503 (2008).

²⁵J. L. Cohn *et al.*, *Phys. Rev. Lett.* **66**, 1098 (1991).

²⁶Y. Wang *et al.*, *Nature (London)* **423**, 425 (2003).